Catalytic Mechanism of Yeast Adenosine 5′-Monophosphate Deaminase. Zinc Content, Substrate Specificity, pH Studies, and Solvent Isotope Effects†

David J. Merkler‡ and Vern L. Schramm*

Department of Biochemistry, Albert Einstein College of Medicine, 1300 Morris Park Avenue, Bronx, New York 10461

Received January 21, 1993; Revised Manuscript Received March 26, 1993

ABSTRACT: Adenosine 5′-monophosphate (AMP) deaminase from baker's yeast is an allosteric enzyme containing a single AMP binding site and two ATP regulatory sites per polypeptide [Merkler, D. J., & Schramm, V. L. (1990) *J. Biol Chem. 265*, 4420–4426]. The enzyme contains 0.98 ± 0.17 zinc atom per subunit. The X-ray crystal structure for mouse adenosine deaminase shows zinc in contact with the attacking water nucleophile using purine riboside as a transition-state inhibitor [Wilson, D. K., Rudolph, F. B., & Quiocho, F. A. (1991) *Science 252*, 1278–1284]. Alignment of the amino acid sequence for yeast AMP deaminase with that for mouse adenosine deaminase demonstrates conservation of the amino acids known from the X-ray crystal structure to bind to the zinc and to a transition-state analogue. On the basis of these similarities, yeast AMP deaminase is also proposed to use a Zn^{2+}-activated water molecule to attack C6 of AMP with the displacement of NH_3. The pK_m and pK_i profiles for AMP and a competitive inhibitor overlap in a bell-shaped curve with pK_a values of 7.0 and 7.4. This pattern is characteristic of a rapid equilibrium between AMP and the enzyme, thus confirming the rapid equilibrium random kinetic patterns [Merkler, D. J., Wali, A. S., Taylor, J., Schramm, V. L. (1989) *J. Biol. Chem. 264*, 21422–21430]. The V_{max} of the reaction requires one unprotonated and one protonated group with pK_a values of 6.4 ± 0.2 and 7.7 ± 0.3, respectively. The ^2H_2O-induced shifts of the pK_a values for these groups are consistent with a carboxylate and a histidine, groups known to be in contact with purine riboside in the adenosine deaminase structure. The V_{max}/K_m profile is similar except that the pK_a values are 6.7 and 7.3, respectively. Kinetic studies with ^2H_2O as solvent gave inverse V_{max}/K_m solvent deuterium isotope effects, i.e., reaction rates more rapid in ^2H_2O than H_2O. Solvent ^2H_2O isotope effects varied from 0.79 ± 0.11 to 0.33 ± 0.03, with the slowest substrates giving the largest isotope effects. Proton inventory studies with a slow substrate indicated that two or more protons give rise to the solvent isotope effect. The results are interpreted in a mechanism where equilibrium proton transfers from the zinc-bound water and/or a compressed hydrogen bond to the substrate contribute to the observed inverse solvent isotope effect.

Adenosine 5′-monophosphate (AMP) deaminase (AMP aminohydrolase, EC 3.5.4.6) catalyzes the irreversible deamination of AMP to IMP and ammonia. ATP is an allosteric activator, and GTP and inorganic phosphate are allosteric inhibitors. The enzyme plays a role in adenine nucleotide

$$AMP + H_2O \xrightarrow[-GTP,\ -PO_4]{+ATP} IMP + NH_3$$

catabolism (Bontemps et al., 1986; Szondy & Newsholme, 1989; Merkler et al., 1989), in the maintenance of the adenylate energy charge (Chapman & Atkinson, 1973; Manfredi & Holmes, 1984; Yoshino & Murakami, 1981, 1985), and in forming substrate for base-exchange reactions (Nygaard, 1983; Hanson et al., 1990). AMP deaminase is one of the three enzymes which make up the purine nucleotide cycle (Lowenstein, 1972). The purine nucleotide cycle produces fumarate, which plays an anaplerotic role for the TCA cycle, and ammonia, which buffers lactate formation during exercise (Zoref-Shani et al., 1983). Patients deficient in AMP deaminase fatigue easily and often exhibit severe neurological and rheumatological symptoms (Sabina et al., 1992). Adenosine is a known cardioprotective agent (Newby, 1984; Bolling et al., 1990) whose levels in the heart are regulated by the AMP concentration and the balance between the activities of 5′-nucleotidase and AMP deaminase (Berne, 1980; Smolenski et al., 1992). Since AMP deaminase shunts adenylate nucleotides away from adenosine to IMP (Smolenski et al., 1992), AMP deaminase inhibitors could have therapeutic value. An understanding of the chemical mechanism for AMP deaminase may facilitate the development of such inhibitors.

Previous work on yeast AMP deaminase has characterized its kinetic and regulatory properties (Murakami, 1979; Yoshino et al., 1979; Yoshino & Murakami, 1980, 1986, 1988; Merkler et al., 1989) and has shown that the enzyme derives its allosteric properties from differential catalytic activity rather than from cooperative substrate binding (Merkler & Schramm, 1990). The yeast enzyme is potently inhibited ($K_m/K_{is} \geq 10^4$) by purine nucleotide analogues that contain a tetrahedral secondary alcohol at a position equivalent to the C6 position of the adenine ring (Merkler et al., 1990). These inhibitors are proposed to mimic the transition state that results from the direct attack of water at C6 of AMP (Frieden et al., 1979).

The X-ray crystal structure of mouse adenosine deaminase has identified the amino acids which are in contact with the enzyme-bound zinc and the C6 hydrate of purine riboside (Wilson et al., 1991). Sequence comparison between yeast AMP deaminase (Meyer et al., 1989) and mouse adenosine deaminase (Yeung et al., 1985) reveals that every amino acid in contact with zinc, the attacking H_2O, and the purine riboside is conserved. This conservation is remarkable since yeast AMP

† This work was supported by a research grant (GM21083) and a postdoctoral fellowship (GM10599) from the National Institutes of Health.

* Address correspondence to this author.

‡ Current address: Analytical Protein & Organic Chemistry Group, Unigene Laboratories, Inc., 110 Little Falls Road, Fairfield, NJ 07004.

0006-2960/93/0432-5792$04.00/0

deaminase contains an 810 amino acid monomer while the adenosine deaminase has only 352 amino acids. Chemical modification, kinetic, and isotope effect studies with adenosine deaminase originally suggested a reactive cysteine; however, this mechanism was revised when no cysteine was found in the catalytic site in the crystal structure and an active-site zinc was revealed (Ronca et al., 1967; Weiss et al., 1987; Wilson et al., 1991; Cleland, 1992).

Studies on yeast AMP deaminase have the advantage of the X-ray crystal structure from mouse adenosine deaminase. Together with results that demonstrate that yeast AMP deaminase is a zinc metalloenzyme, a mechanism is proposed which accounts for observed pK_a values, solvent deuterium isotope effects, and substrate specificity. In contrast to the results obtained with adenosine deaminase (Weiss et al., 1987; Cleland, 1992), a minimum of two proton transfers gives rise to the observed solvent isotope effects for AMP deaminase. The results are consistent with the equilibrium transfer of several protons, which involves the zinc-bound water and/or protonation of the substrate.

MATERIALS AND METHODS

Materials. Bakers' yeast AMP deaminase was purified by the method of Merkler et al. (1989). Unless otherwise noted, specific activities exceeded 450 μmol/min/mg for all enzyme preparations when assayed at 30 °C. This form of the enzyme is missing the 192 N-terminal amino acids (Meyer et al., 1989). ^2H_2O was from Aldrich or Cambridge Isotope Laboratories. Aqueous ethylamine (70%) was from Eastman Kodak. Nucleosides and nucleotides were of the highest grade available from Sigma, Aldrich, or Calbiochem. 2′,3′-Dialdehyde-AMP was prepared by the periodate cleavage of AMP (Easterbrook-Smith et al., 1976). Purine riboside 5′-monophosphate was prepared by the phosphorylation of purine riboside with adenosine kinase (Merkler & Schramm, 1987). Ribavirin 5′-monophosphate was prepared by the phosphorylation of ribavirin (Streeter et al., 1973). The ^{31}P NMR spectra of both purine 5′-monophosphate and ribavirin 5′-monophosphate gave a single triplet peak, indicating that the phosphate is esterified only to the 5′-hydroxyl. 8-Bromo-AMP was synthesized from AMP essentially by the method of Lowe (1977), except that the addition of $Na_2S_2O_5$ was found unnecessary and was omitted. 8-Mercapto-AMP (Ikehara, 1973) and 8-(ethylamino)-AMP (Long et al., 1967) were synthesized from 8-bromo-AMP and subsequently purified and crystallized according to published procedures. Ocassionally, the final nucleotide product would not crystallize. In such cases, the nucleotide was loaded onto a Dowex AG1X-8 column, washed with H_2O, and eluted with a linear gradient of acetic acid. The resulting nucleotide could then be crystallized. The crystallized nucleotides gave single, symmetric HPLC peaks and had the appropriate UV characteristics.

Initial Rate Studies. Deamination of AMP to IMP and NH_3 was measured using the spectrophotometric assay previously described (Merkler et al., 1989) or the colorimetric assay for ammonia (Chaney & Marbach, 1962). The buffer for enzyme assays was 30 mM HEPES (pH 7.0) or 50 mM triethanolamine hydrochloride (pH 7.0), 100 mM KCl, 100 μM DTT, and 100 μM ATP. For solvent isotope effect studies, the assay mix without nucleotides was lyophilized to dryness and resuspended in the appropriate volume of ^2H_2O. Stocks of nucleotides were prepared in ^2H_2O. No change in the $\Delta\epsilon$ for the conversion of AMP to IMP was observed upon changing H_2O to ^2H_2O.

Measurement of the kinetic constants as a function of pH was achieved in assay mixtures containing 25 mM each of potassium acetate, MES, HEPES, and CAPS plus 100 mM KCl adjusted to the desired pH with KOH. In some experiments, 100 μM ATP was also included. Previous studies have established that free ATP activates the enzyme; thus, magnesium salts were not added. Measurement of the kinetic constants as a function of pD was accomplished by lyophilizing the assay mix of the appropriate pD (pH meter reading +0.4) and resuspending the mix in ^2H_2O. The pH and pD values were measured before and after the assays were performed and were found to vary by ≤0.1 pH(D) unit.

Determination of Zinc Stoichiometry. Enzyme was exhaustively dialyzed into 30 mM HEPES (pH 7.0), 100 mM KCl, 100 μM DTT, and 100 μg/mL NaN_3. The dialysis buffer was used to zero the atomic absorption spectrometer and to construct the zinc standard curve. Zinc was determined by flame ionization on a Perkin-Elmer 4000 atomic absorption spectrometer or on a Perkin-Elmer 5000 spectrometer equipped with a graphite furnace according to the manufacturer's directions. Protein was determined using the Bradford dye binding assay, which was calibrated by dry weight analysis of the protein (Merkler et al., 1990).

Analysis of Kinetic Data. Kinetic data were analyzed using the computer programs of Cleland (1979). The data were fit to eqs 1–3 when visual inspection indicated linear double-reciprocal plots of initial velocity, linear competitive, or noncompetitive inhibition, respectively.

$$v = V_{max}A/(K_m + A) \quad (1)$$

$$v = V_{max}A/\{K_m[1 + (I/K_{is})] + A\} \quad (2)$$

$$v = V_{max}A/\{K_m[1 + (I/K_{is})] + A[1 + (I/K_{ii})]\} \quad (3)$$

Kinetic data which result in curvilinear double-reciprocal plots were fit to eqs 4 and 5 using an iterative procedure.

$$v = V_{max}A^n/(K' + A^n) \quad (4)$$

$$S_{0.5} = 10^{(\log K'/n)} \quad (5)$$

pH(D) profiles in which the log of the parameter (V or V_{max}/K_m) decreased both above pK_2 with a slope of −1 and below pK_1 with a slope of 1 were fit to eq 6 where C is the pH(D)-independent plateau value.

$$\log y = \log \{C/(1 + [H^+]/K_1 + K_2/[H^+])\} \quad (6)$$

RESULTS

Zinc Stoichiometry. The zinc content of yeast AMP deaminase is shown in Table I. A value of 0.98 ± 0.17 zinc atom/subunit agrees with the recent discovery of an atom of zinc in the active site of adenosine deaminase (Wilson et al., 1991).

Substrate Specificity of AMP Deaminase. Of the analogues tested, AMP had the highest V_{max}/K_m value of the substrates for yeast AMP deaminase. Additional nucleotides which were active as substrates include variants in both ribose and base and are summarized in Table II. Modifications to the adenine or ribose ring substantially decreased V_{max}/K_m for the AMP analogues. The best alternate substrates, N^6-CH_3-AMP and ara-AMP, had V_{max}/K_m values which were approximately 2% of that measured for AMP. Replacement of the 5′-phosphate with a 5′-sulfate permitted a significant rate of catalysis, ~40% of the V_{max} of AMP. However, the 170-fold

Table I: Zinc Stoichiometry

expt	[subunit][a] (μM)	[zinc] (μM)	zinc/subunit
I[b]	10.4	12.5	1.2
I	10.5	9.2	0.9
I	9.1	11.3	1.2
II[c]	2.8	2.5	0.9
II	7.8	6.9	0.9
II	14.1	11.9	0.8
			av 0.98 ± 0.17

[a] Based on a subunit molecular mass of 80 000 kDa. [b] Determined by flame ionization on a Perkin-Elmer Model 4000 atomic absorption spectrometer. Samples I and II are from two separate enzyme preparations. [c] Determined using a carbon rod furnace in a Perkin-Elmer Model 5000 atomic absorption spectrometer.

increase in K_m for adenosine 5′-monosulfate to 52 ± 16 mM results in a value of V_{max}/K_m which is only ~0.2% that of AMP. Substitution of the 5′-monophosphate with a 5′-diphosphate or -triphosphate also permitted catalysis, but the large increases in K_m and decreases in V_{max} gave V_{max}/K_m values only 7.3×10^{-5} that of AMP for ADP and 4×10^{-7} that of AMP for ATP as substrate.

Inhibitor Specificity of AMP Deaminase. The specificity for inhibitors of AMP deaminase is narrow. Ribose 5-monophosphate, (methylthio)adenosine, and many nucleotides including GMP, TMP, ribavirin 5′-monophosphate, 1-methyl-AMP, and 6-chloropurine riboside 5′-monophosphate gave no inhibition at concentrations above 5 mM with AMP concentration fixed at its K_m value. Substrate recognition therefore depends on the groups which are involved in catalysis. Replacement of the 6-amino with 6-mercapto or 6-chloro inhibits binding, as does methylation of N1. Purine riboside 5′-monophosphate, N^6-methyl-AMP, 8-mercapto-AMP, and 8-(ethylamino)-AMP are competitive inhibitors that bind to enzyme 2–3-fold tighter than substrate (Table II). The tight binding of coformycin and deoxycoformycin analogues to yeast AMP deaminase was described previously (Merkler et al., 1990).

Effect of pH on the Kinetic Constants for AMP and N^6-Methyl-AMP. Changes in V_{max} and $V_{max}/S_{0.5}$ for AMP as a function of pH and solvent are shown in Figure 1. These results were obtained in the absence of allosteric activation by ATP at pH values above 6.0, where AMP interacts in a cooperative manner with AMP deaminase. Below pH 6.0, AMP shows normal Michaelis–Menten behavior independent of ATP, and results were obtained both in the absence and presence of ATP at lower pH values. The V_{max} pH(D) profiles indicate pK_a values of 6.4 ± 0.2 and 7.7 ± 0.3 in H_2O and 7.3 ± 0.3 and 8.2 ± 0.3 in ^2H_2O, with limiting slopes of 1.0. The pK_a values from the $V_{max}/S_{0.5}$ pH(D) profiles were 6.7 ± 0.04 and 7.3 ± 0.4 in H_2O and approximately 7.5 and 7.9 in ^2H_2O, with limiting slopes of 1.0. Because the pK_a values obtained from the $V_{max}/S_{0.5}$ pD profiles are only separated by ~0.4 pD unit, the data cannot be unambiguously fit to eq 6. Consequently, these pK_a values are approximate.

The pH profiles of the K_m values for AMP and the K_{is} values for N^6-methyl-AMP were obtained in the presence of

Table II: Comparison of K_m, K_{is}, V_{max}, and V_{max}/K_m Values for AMP Analogue Interactions with AMP Deaminase[a]

	K_m (μM)	K_{is}[b] (μM)	V_{max}[c] (μmol/min/mg)	V_{max}/K_m (s^{-1} M^{-1})
substrates				
AMP	300 ± 10		627 ± 155[d]	$(2.6 \pm 0.7) \times 10^6$
N^6-CH_3-AMP	111 ± 17		~6	6.7×10^4
ara-AMP	690 ± 20		31.7 ± 0.4	$(5.7 \pm 0.2) \times 10^4$
2′,3′-dialdehyde-AMP	490 ± 40		10.8 ± 0.4	$(2.8 \pm 0.2) \times 10^4$
2′-dAMP	1200 ± 40		23.0 ± 0.4	$(2.4 \pm 0.1) \times 10^4$
adenosine 5′-monosulfate	52000 ± 16000		246 ± 69	$(5.9 \pm 2.5) \times 10^3$
3′-dAMP	770 ± 70		3.1 ± 0.1	$(5.0 \pm 0.5) \times 10^3$
8-bromo-AMP[e]	350 ± 20		0.9 ± 0.02	$(3.3 \pm 0.2) \times 10^3$
ADP	3000 ± 900		0.5 ± 0.07	$(1.9 \pm 0.7) \times 10^2$
tubercidin 5′-monophosphate[f]	1300 ± 100	1500 ± 300	0.08 ± 0.004	73 ± 9
ATP[g]	~57000		~0.04	~1
inhibitors				
N^6-CH_3-AMP		154 ± 18[h]	see above	
8-SH-AMP		119 ± 17	<0.05	
		163 ± 13[i]		
8-(ethylamino)-AMP		129 ± 9	<0.02	
purine riboside 5′-monophosphate		155 ± 11[i]	0	
GMP		>5000		
TMP		>5000		
ribose 5-phosphate		>5000		
(methylthio)adenosine		>5000		
1-CH_3-AMP		>5000	<0.03	
6-mercaptopurine 5′-monophosphate		>5000	<0.003	
ribavirin 5′-monophosphate		>5000		
6-chloropurine riboside 5′-monophosphate		>5000		

[a] Kinetic constants are reported as the weighted mean ± standard error (Morrison & Uhr, 1966). A value of >5000 μM indicates that no inhibition was detected at 1.0 mM inhibitor and 500–600 μM AMP. Assay mixtures contained 100 μM ATP. In the absence of ATP, the kinetics are non-Michaelis–Menten. [b] Except where indicated, the inhibition patterns were slope–linear competitive. Values of K_{is} were determined by fits of the experimental data to eq 2 or 3. [c] Where no value for V_{max} is listed, no substrate activity could be detected at inhibitor concentrations of 1.0 mM under conditions which would detect a rate of <1 μmol/min/mg. [d] V_{max} values varied with the age of the enzyme preparation. This value is the mean for six determinations ± standard deviation from four different enzyme preparations. Under these conditions (see Materials and Methods), the highest value for V_{max} obtained was 886 μmol/min/mg. [e] At concentrations >2 mM, apparent substrate inhibition occurred for 8-bromo-AMP. The data conformed to simple substrate inhibition, $v = V_{max}A/\{K_m + A(1 + A/K_i)\}$, with a K_i value of 37 ± 5 mM. [f] Tubercidin 5′-monophosphate was a noncompetitive inhibitor vs AMP. Data were fit to eq 3 yielding a K_{is} value as shown and a K_{ii} = 4.8 ± 1.0 mM. The specific activity for the enzyme used for the tubercidin 5′-monophosphate inhibition studies was 91 ± 3 μmol/min/mg. [g] Deamination of ATP to ITP was monitored using the HPLC system (Merkler & Schramm, 1987). All initial rates were obtained at substrating ATP (2–40 mM); therefore, the kinetic constants for ATP are approximate. [h] Obtained at 4 °C, where catalysis is less than 1% of that occurring with AMP as substrate. [i] Apparent K_{is} obtained by varying the inhibitor concentration at constant AMP.

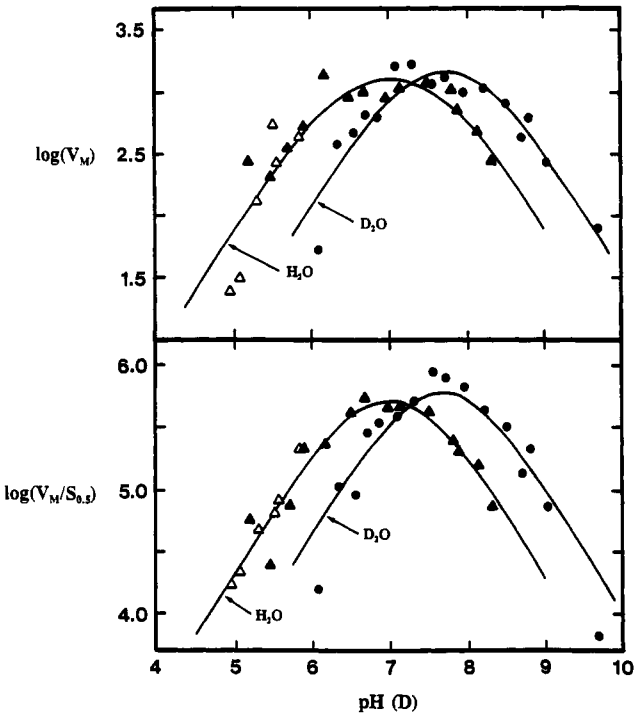

FIGURE 1: pH(D) profiles for AMP: data for ^2H_2O (D_2O) (●); data for H_2O (△, ▲). The curves in the figure are drawn from fits of V_{max} or $V_{max}/S_{0.5}$ to eq 6. The V_{max} and $V_{max}/S_{0.5}$ values were measured at 30 °C in a mixed buffer system consisting of 25 mM each potassium acetate, MES, HEPES, and CAPS, 100 mM KCl, and 100 μM DTT, adjusted to the indicated pH with KOH. In a few experiments in H_2O, 100 μM ATP was included (△).

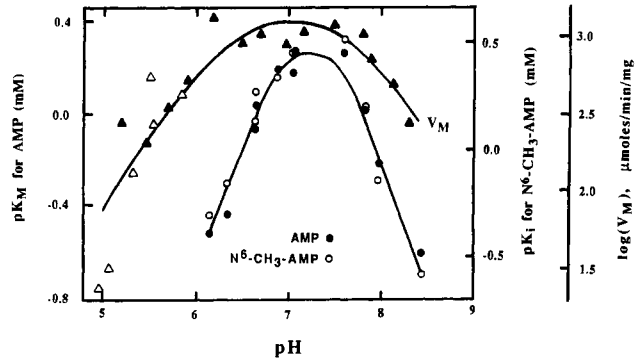

FIGURE 2: Comparison of the V_{max} and K_m values for AMP and the K_{is} values for N^6-CH_3-AMP as a function of pH. The values for V_{max} are the same as those used in Figure 1 in the presence of H_2O. Since V_{max} is independent of ATP (Merkler et al., 1989), omission of ATP does not affect the V_{max} values. The curve for the V_{max} data (△, ▲) is drawn from a fit to eq 6. For the pK_m and pK_i determinations, reactions were initiated at 30 °C by the addition of enzyme into a mixed buffer system containing 25 mM each potassium acetate, MES, HEPES, and CHAPS, 100 mM KCl, 100 μM ATP, and 100 μM DTT, adjusted to the indicated pH with KOH. The curve for the K_m for AMP and the K_{is} for N^6-CH_3-AMP (○, ●) has pK_a values too close to permit analysis by eq 6. The line is drawn by eye to fit the experimental points.

ATP to provide linear double-reciprocal plots as a function of AMP concentration and are shown in Figure 2. The pK_a values from both the K_m and K_{is} are approximately 7.0 and 7.4, with slopes equal to or greater than 1.0. Since the pK_a values are separated by only ~0.4 pH unit, an exact determination of the pK_a values according to eq 6 is not possible. However, the data clearly demonstrate that the pK_m and pK_{is} curves overlap and differ considerably from the V_{max} curve.

Solvent Isotope Effects. Values for $^{D_2O}V_{max}$ and $^{D_2O}(V_{max}/K_m)$ of 0.98 ± 0.04 and 0.71 ± 0.07 for AMP, respectively, were obtained in the absence of ATP, the allosteric activator. In the presence of 100 μM ATP, the $^{D_2O}V_{max}$ decreased to 0.75 ± 0.03 while the $^{D_2O}(V_{max}/K_m)$ was unchanged, 0.79 ± 0.11. With dAMP as a substrate, the $^{D_2O}V_{max}$ and $^{D_2O}(V_{max}/K_m)$ values were 0.62 ± 0.02 and 0.49 ± 0.04 in the absence of ATP. ATP (100 μM) decreased the $^{D_2O}(V_{max}/K_m)_{dAMP}$ value to 0.34 ± 0.02 while the $^{D_2O}V_{dAMP}$ value was unchanged at 0.63 ± 0.02. The $^{D_2O}V_{BrAMP}$ and $^{D_2O}(V_{max}/K_m)_{BrAMP}$ values obtained in the presence of 100 μM ATP, 0.58 ± 0.03 and 0.33 ± 0.03, are similar to those measured for dAMP as a substrate. The solvent isotope effects are summarized in Table III. A plot of initial rate determined at 100 μM dAMP in the absence of ATP vs the mole fraction of ^2H_2O is shown in Figure 3. The solid line represents the fit to the Gross–Butler equation for a diprotonic transition state with $(\text{initial rate})_H/(\text{initial rate})_D = 0.26$, while the dashed line represents the fit for a monoprotonic transition state (cf. Quinn and Sutton (1991)). The observed inverse ^2H_2O isotope effect of 0.26 from Figure 3 agrees well with that predicted from the kinetic constants listed in Table III, where the ratio of the initial rate in H_2O to that in ^2H_2O at 100 μM dAMP and no ATP should be 0.27.

DISCUSSION

Previous studies of yeast AMP deaminase have centered around the kinetic and regulatory properties of the enzyme (Murakami, 1979; Yoshino et al., 1979; Yoshino & Murakami, 1980, 1986, 1988; Merkler & Schramm, 1990) and its role in adenine nucleotide metabolism (Yoshino & Murakami, 1981, 1985; Merkler et al., 1989; Smolenski et al., 1992). In contrast to adenosine deaminase, little mechanistic work has been carried out for yeast AMP deaminase. On the basis of the slow, tight binding inhibition of AMP deaminases by coformycin 5′-monophosphate and related analogues (Frieden et al., 1980; Merkler et al., 1990), it seems likely that the transition state has substantial tetrahedral character or a transient tetrahedral intermediate forms following the attack of water on the C6 of AMP. Substrate and inhibitor specificities, metal content of the enzyme, pH variation kinetics, and solvent ^2H_2O isotope effects have been analyzed in the context of the X-ray crystal studies with mouse adenosine deaminase (Wilson et al., 1991). Together, these results provide new understanding of the deamination catalyzed by yeast AMP deaminase.

Homology between Yeast AMP Deaminase and Mouse Adenosine Deaminase. The X-ray crystal structure for mouse adenosine deaminase provides a guide for the amino acids in contact with a transition-state analogue of adenosine and the zinc atom responsible for activation of the water nucleophile (Wilson et al., 1991). A schematic drawing of these contacts is shown in Figure 4. Alignment of these amino acid residues with the deduced amino acid sequence for yeast AMP deaminase indicated that every amino acid side chain in contact with the zinc, purine base, and ribose is conserved in AMP deaminase with similar spacing on the peptide chain. An exception is the Gly184 of adenosine deaminase, which is in contact with N3 of the purine riboside. However, this contact is with the peptide backbone; thus, the Tyr601 which occupies this position in yeast AMP deaminase can make a similar contact. Thus, every amino acid contact is conserved. The catalytic site of yeast AMP deaminase is located near the C-terminal end of the protein of 810 amino acids, with the region of amino acids 422–708 corresponding to amino acids 15–296 of the 352 amino acids of mouse adenosine deaminase

Table III: Solvent Isotope Effects for AMP Deaminase[a]

substrate	solvent	ATP[b] (μM)	K_m or $S_{0.5}$ (mM)	V_{max} (μmol/min/mg)	n[c]	$^{D_2O}V_{max}$	$^{D_2O}(V_{max}/K_m)$ or $^{D_2O}(V_{max}/S_{0.5})$
AMP	H_2O	0	1.8 ± 0.1	636 ± 22	1.9		
						0.98 ± 0.04	0.71 ± 0.07
	D_2O	0	1.3 ± 0.1	647 ± 15	1.6		
	H_2O	100	0.20 ± 0.03	648 ± 23	1.0		
						0.75 ± 0.03	0.79 ± 0.11
	D_2O	100	0.21 ± 0.03	859 ± 26	1.0		
2′-dAMP	H_2O	0	2.3 ± 0.1	14.0 ± 0.2	1.8		
						0.62 ± 0.02	0.49 ± 0.04
	D_2O	0	1.8 ± 0.1	22.5 ± 0.8	1.7		
	H_2O	100	1.2 ± 0.04	22.8 ● 0.3	1.0		
						0.63 ± 0.02	0.34 ± 0.02
	D_2O	100	0.64 ± 0.05	34.9 ± 1.0	1.0		
8-bromo-AMP	H_2O	100	0.35 ± 0.02	0.91 ± 0.02	1.0		
						0.58 ± 0.03	0.33 ± 0.03
	D_2O	100	0.20 ± 0.02	1.55 ± 0.03	1.0		

[a] Kinetic constants are reported as the weighted mean ± standard error (Morrison & Uhr, 1966). [b] ATP concentration included in the assay. [c] Hill coefficient.

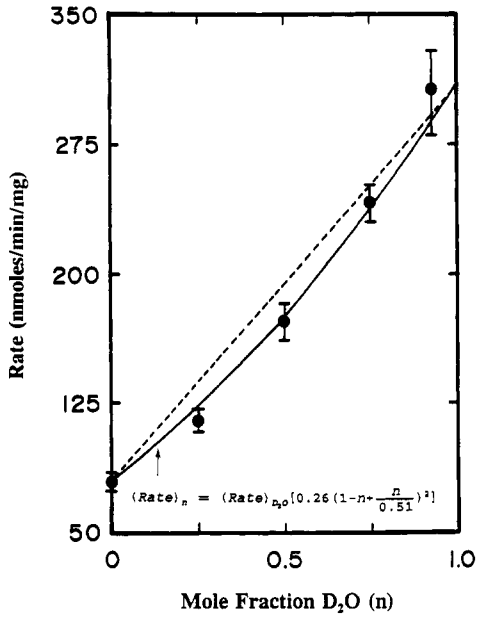

FIGURE 3: Proton inventory for V_{max}/K_m with 2-deoxy-AMP as a substrate. Reactions were initiated at 30 °C by the addition of 50 μg of enzyme (specific activity = 430 μmol/min/mg) into 1.0 mL of 30 mM HEPES (pH 7.0), 100 mM KCl, 100 μM DTT, and 100 μM dAMP. The concentration of dAMP used was approximately 20-fold below the $S_{0.5}$ (Table III); thus, the initial rate closely approximates the V_{max}/K_m. The mole fraction of D_2O was varied from 0 to 93%.

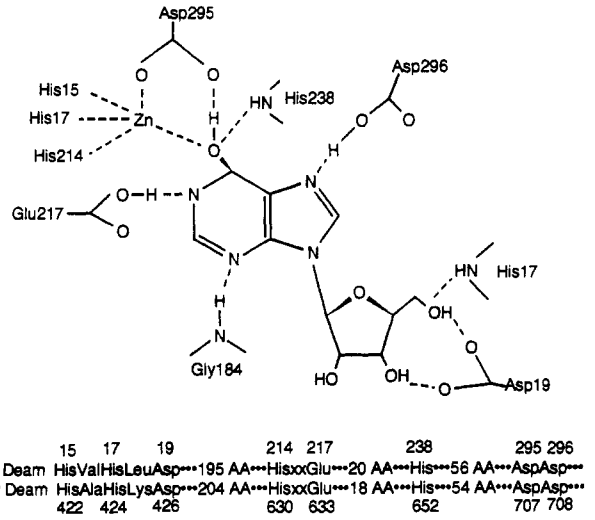

FIGURE 4: Schematic position of purine riboside in the crystal structure of mouse adenosine deaminase and amino acid homology with yeast AMP deaminase. The contacts to purine riboside are from Wilson et al. (1991). Below the purine riboside is the amino acid alignment of groups proposed to stabilize AMP at the catalytic site of yeast AMP deaminase.

(Yeung et al., 1985; Meyer et al., 1989). The N-terminal 1–421 amino acid region of yeast AMP deaminase is larger than the catalytic domain and must provide for the allosteric interactions by binding 2 mol of ATP per subunit. This function is absent in adenosine deaminase.

On the basis of the amino acid similarity between adenosine deaminase and AMP deaminase at the catalytic sites, a model can be proposed for binding and catalytic amino acids for AMP deaminase (Figure 5). Amino acids proposed to play a role unique to AMP deaminase are included. Three groups are critical in accomplishing the hydrolytic deamination. Zinc activates the attacking water nucleophile, while Asp707 promotes protonic transfer from the activated water to the departing ammonia *or* it acts as a bridge to transfer the proton to His652 after His652 transfers its proton to the departing NH_3. Rehybridization of C6 of the purine from sp^2 to sp^3 causes N1 to become strongly electronegative, causing protonation or charge stabilization by hydrogen bonding to Glu633. The arrangement of groups involved in catalysis is discussed below.

Substrate and Inhibitor Specificity. Alterations in the ribofuranose ring, the monophosphate ester, or the adenine ring of AMP reduce catalytic efficiency, in agreement with the results obtained with AMP deaminases from other sources (rabbit muscle, Zielke and Suelter (1971), and human erythrocyte, Yun and Suelter (1978)). Of the compounds tested, ara-AMP and N^6-methyl-AMP have the highest V_{max}/K_m values, approximately 2% of that for AMP. The active-site His424 and Asp426 form hydrogen bonds with specific ribosyl hydroxyls, accounting for the low V_{max}/K_m values for 2′,3′-dialdehyde-AMP, 2′-deoxy-AMP, and 3′-deoxy-AMP. The active site also contains Lys425, which provides specificity for the 5′-monophosphate. Adenosine binds poorly and is not a significant substrate. Excess negative charge as in ADP and ATP also results in small V_{max}/K_m values. The phosphate subsite is specific for the ionization state since the relative V_{max}/K_m value for adenosine 5′-monosulfate is only 0.2%, and (methylthio)adenosine, with a 5′-CH_3S group, is not deaminated under the conditions of these experiments. Adenosine specificity in adenosine deaminase is provided by the interaction of the 3′- and 5′-hydroxyls with His17 and Asp19, where the intervening amino acid is Leu18. In contrast,

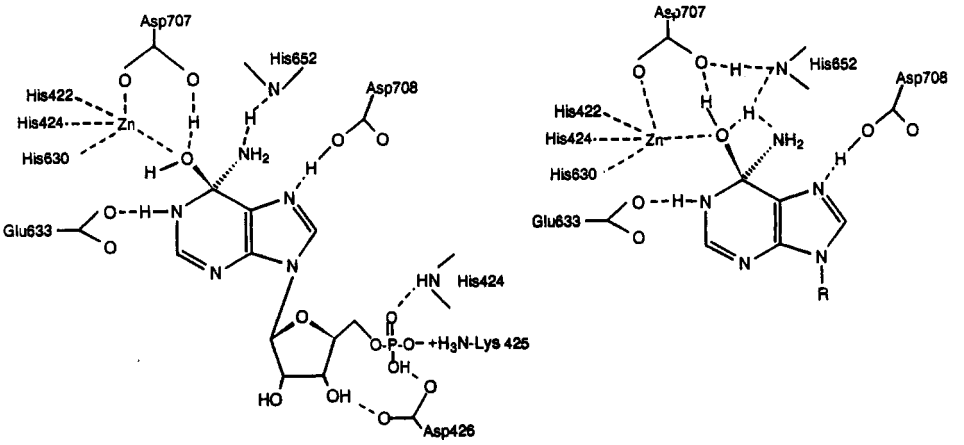

FIGURE 5: Proposed interactions of AMP transition states at the catalytic site of yeast AMP deaminase. The structures provide two hypothetical bonding schemes based on the adenosine deaminase structure (Wilson et al., 1991) and the homology to AMP deaminase shown in Figure 4.

the intervening amino acid for AMP deaminase is Lys425, which is likely to be involved in ion pairing with the 5′-phosphate of AMP (Figure 5).

AMP analogues substituted with Cl or HS at the C6 position failed to bind to AMP deaminase. This result differs from the facile hydrolysis of these groups by adenosine deaminase [cf. Wolfenden et al. (1969)]. The result establishes that the 6-amino group is recognized to form the Michaelis complex prior to the attack of zinc-activated H_2O. The groups which interact with the 6-amino are not apparent from the X-ray crystal structure of adenosine deaminase (Wilson et al., 1991); however, Glu217 and Asp295, which correspond to Glu633 and Asp707, respectively, in AMP deaminase, appear to be nearest neighbors when a tetrahedral intermediate is considered.

Analogues substituted in the C8 position with bromo, mercapto, or ethylamino groups are good inhibitors of yeast AMP deaminase with $K_{is}/K_m \leq 1.2$, but they are poor substrates. Since these compounds bind 1–3-fold more tightly than AMP, the C8 substituents permit binding but prevent the enzyme·nucleotide complex from reaching the transition state. The crystal structure of mouse adenosine deaminase complexed with a transition-state analogue demonstrates that a loop folds over the C8 region of adenosine (Wilson et al., 1991). Prevention of this protein motion, therefore, causes inefficient catalysis. Wilson et al. (1991) found that the N7 of adenosine forms a hydrogen bond important for interaction with the transition-state analogue. Since N7 is replaced with a carbon atom in tubercidin 5′-phosphate, this hydrogen bond cannot form. This result establishes that the hydrogen bond to N7 is required for efficient catalysis since the V_{max}/K_m value for tubercidin 5′-monophosphate is 3×10^{-5} that for AMP. The mechanism for adenosine deaminase has been proposed to involve protonation of N1 by Glu217 (Wilson et al., 1991; Cleland, 1992), which would be required as C6 is converted from an sp^2 to an sp^3 hybridization. The lack of binding or substrate activity for 1-CH_3-AMP indicated that the methyl group prevents binding to the enzyme.

pH Profiles and the Effect of ^2H_2O. Using AMP as a substrate, the V_{max} and $V_{max}/S_{0.5}$ profiles showed decreased activity at both low and high pH, with pK_a's of 6.5 ± 0.2 and 7.5 ± 0.3 and limiting slopes of unity (Figure 1). These pK_a values are consistent with a single unprotonated carboxylate in a hydrophobic environment and a protonated imidazole, which are required for catalysis. Since similar pK_a's are seen in the V_{max} and $V_{max}/S_{0.5}$ profiles, AMP binding induces only small perturbations in the ionization of these groups. When H_2O is replaced with ^2H_2O, the pK_a values for V_{max} and $V_{max}/S_{0.5}$ increase to approximately 7.3 and 8.1, also consistent with the involvement of a carboxylate and an imidazole (Quinn & Sutton, 1991).

The ionizable groups of Figure 5 which readily correlate with the pK_a and ^2H_2O effects are Asp707 and His652. In the crystal structure for adenosine deaminase, the corresponding groups are unprotonated and protonated, respectively, and would clearly be required for catalysis. In the adenosine deaminase mechanism proposed by Wilson et al. (1991), Asp295 abstracts a proton from the attacking water nucleophile while remaining coordinated to the zinc through the other carboxylate oxygen. The histidine is proposed to hydrogen bond to the attacking oxygen while remaining protonated through the catalytic cycle.

Binding of substrate or the slow substrate N^6-methyl-AMP requires an unprotonated group with a pK_a near 7.0 and a protonated group with pK_a near 7.4. Conversion of either to the inappropriate protonation state abolishes binding (Figure 2). The substrate analogues GMP, 7-deaza-AMP, 5′-(methylthio)adenosine, 1-methyl-AMP, and 6-chloropurine riboside 5′-monophosphate have features which abolish binding since all have K_i values >5 mM. These modifications disrupt interactions between (1) the N^6-amino group and His652, (2) N7 and Asp708, (3) the 5′-phosphate and His424, Lys425, and Asp426, and (4) the N1 interaction with Glu633. Candidates for these binding interactions include four ionizable groups from the amino acids which contact the substrate. In addition, the phosphate group has a pK_a value in the range obtained in the V_{max}, $S_{0.5}$, and K_m profiles. Two groups consistent with the pK_a profile for the K_m for AMP and the K_i for N^6-methyl-AMP are Asp426 and His424, which are involved in ribose 5-phosphate recognition and have the appropriate ionization states. Disruption of these contacts would clearly interfere with binding. Glu633 is less likely to appear in the pK_a profile for substrate binding since 1-deazaadenosine binds more tightly than substrate to adenosine deaminase (Kurz et al., 1992). The relatively tight binding of purine riboside 5′-phosphate to AMP deaminase indicates that the Asp707 and His652 contacts are not likely to appear in the pH profiles for substrate binding.

The limiting slopes for the pH profiles in Figures 1 and 2 are near unity. This observation is remarkable with eight ionizable amino acids in addition to the 5′-phosphate of AMP involved at the catalytic site of AMP deaminase. Obviously, the high- and low-pH limbs of the pH profiles in Figures 1 and 2 provide only apparent slopes of unity because of the

limited pH ranges and the inherent inaccuracy of the data.

Commitment to Catalysis for AMP. Enzyme-bound substrates which are committed to catalysis react to yield products at a significant rate compared to the rate of dissociation from the enzyme. Substrates in rapid equilibrium with the enzyme dissociate to the medium more frequently than they convert to products (Cleland, 1977). The binding and release of a competitive inhibitor are at equilibrium in the steady state; thus, overlapping pH profiles for a competitive inhibitor (pK_{is}) and for substrate (pK_m) indicate that the substrate is also in equilibrium with enzyme, provided that the V_{max} profile differs from the pK_{is} plot and that the inhibitor and substrate have the same pK_a's. The pH profiles for the pK_{is} of N^6-methyl-AMP and the pK_m and V_{max} profiles for AMP fit this pattern exactly. The pK_a's for N^6-methyl-AMP (Dawson et al., 1986) and AMP (Martin, 1985) are the same. Thus, AMP is in true equilibrium with the enzyme, further establishing a rapid equilibrium mechanism and illustrating that enzyme-bound AMP has an insignificant commitment to catalysis. This finding is in contrast to the mechanism of adenosine deaminase in which bound adenosine is highly committed, partitioning forward to products more frequently than dissociating (Weiss et al., 1987; Kurz et al., 1992). The finding that AMP is not committed on AMP deaminase is consistent with the lower affinity of AMP, with dissociation constants of 100–1800 μM compared to a K_d of 1–10 μM for adenosine with adenosine deaminase (Kurz et al., 1992).

Solvent ^2H_2O Kinetic Isotope Effects. Solvent isotope effects on the kinetic constants for yeast AMP deaminase (summarized in Table III) are inverse, with reaction rates being accelerated and causing higher substrate affinity in the presence of ^2H_2O. The largest inverse solvent isotope effects are obtained with the slow substrates dAMP and 8-bromo-AMP in the presence of allosteric activation by ATP. Inverse solvent isotope effects can arise from the proton fractionation factors from cysteine or zinc·water complexes (Quinn & Sutton, 1991), from compressed hydrogen bond arrangements between acceptor and donor groups with similar pK_a values (Cleland, 1992), or from differences in the chemical potential of solutes in H_2O relative to ^2H_2O (Kurz et al., 1992). In contrast to these pre-transition-state equilibrium effects, isotope effects arising from proton transfers (protons in motion) at the transition state are expected to give normal isotope effects.

Isotope effects originally attributed to proton donation by cysteine for adenosine and AMP deaminases can be ruled out from the X-ray crystal structure (Wilson et al., 1991). The possibility of a compressed hydrogen bond between N1 of AMP and Glu633 (Figure 5) is analogous to the mechanism proposed for the inverse solvent isotope effects observed with adenosine deaminase (Weiss et al., 1987; Cleland, 1992). This proposal has been questioned for adenosine deaminase by the measurement of solvent deuterium isotope effects of similar magnitudes for the binding of purine ribosides, 1-deazapurine ribosides, and the tight-binding coformycin analogues (Kurz et al., 1992). In addition, the structure of adenosine deaminase with the hydrate of purine riboside shows an oxygen–nitrogen distance of 2.8 Å between Glu217 and N1 of the purine (Wilson et al., 1991). A hydrogen-bonding distance of approximately 2.4 Å or less is required for the magnitude of the inverse solvent isotope effects seen with AMP or adenosine deaminase (Cleland, 1992). Although it can be argued that the hydrogen bond may be tighter in the actual transition state, purine riboside hydrate is thought to bind near the maximum affinity for an ideal transition-state mimic (Jones et al., 1989) and is thus expected to provide a good model for transition-state bonding.

The observed solvent isotope effects thus arise from the protonic transfer(s) which has occurred from the zinc·water and less well defined bulk solvent properties, including altered substrate chemical potential in H_2O and ^2H_2O. The inverse solvent isotope effect of 0.34 on V_{max}/K_m for dAMP contains contributions from both K_m and V_{max} and is larger than expected for bulk solvent effects alone. Proton inventory experiments (Figure 3) indicated that two (or more) proton transfers are involved in the solvent isotope effects. A single proton transfer from zinc·water to a more usual environment is expected to give an inverse effect of approximately 0.75. When combined with the ^2H_2O effect on substrate binding (also observed with adenosine deaminase for substrate analogue binding) (Kurz et al., 1992), these effects could account for an inverse isotope effect near 0.5. However, the values of 0.33 and 0.34 for slow substrates require additional effects and are consistent with the combination of the substrate binding effect in addition to two proton transfers from zinc·water. Two transfers from a zinc·water complex could occur in a proton relay between the zinc-bound water, Asp707, His652 (or another nearby group such as Glu633), and the departing NH_3 as shown schematically in Figure 5. The experimental results cannot eliminate the possibility of a single proton transfer from zinc·water, with a compressed hydrogen bond also giving an additional inverse effect. Additional crystallographic information should prove useful in resolving these mechanisms.

The relatively small inverse solvent ^2H_2O isotope effects with AMP relative to slower substrates indicate that different steps dominate the energetic barriers of the reaction coordinate for AMP, which reacts with a rate approaching 1000 s^{-1} at 30 °C. When groups are optimally aligned for the necessary proton transfers, the reaction coordinate motion could include a proton transfer with a small normal isotope effect to negate the isotope effects resulting from proton transfers which dominate the isotope effects with poor substrates.

REFERENCES

Berne, R. M. (1980) *Circ. Res. 47*, 807–813.

Bolling, S. F., Bies, L. E., Bove, E. L., & Gallagher, K. P. (1990) *J. Thorac. Cardiovasc. Surg. 99*, 469–474.

Bontemps, F., Van den Berghe, G., & Hers, H. G. (1986) *J. Clin. Invest. 77*, 824–830.

Chaney, A. L., & Marbach, E. P. (1962) *Clin. Chem. 8*, 130–132.

Chapman, A. G., & Atkinson, D. E. (1973) *J. Biol. Chem. 248*, 8309–8412.

Cleland, W. W. (1977) *Adv. Enzymol. Relat. Areas Mol. Biol. 45*, 273–387.

Cleland, W. W. (1979) *Methods Enzymol. 63*, 103–138.

Cleland, W. W. (1992) *Biochemistry 31*, 317–319.

Dawson, R. M. C., Elliot, D. C., & Jones, K. M. (1986) *Data for Biochemical Research*, 3rd ed., p 104, Clarendon Press, Oxford, UK.

Easterbrook-Smith, S. B., Wallace, J. C., & Keech, D. B. (1976) *Eur. J. Biochem. 62*, 125–130.

Frieden, C., Gilbert, H. R., Miller, W. H., & Miller, R. L. (1979) *Biochem. Biophys. Res. Commun. 91*, 278–283.

Frieden, C., Kurz, L. C., & Gilbert, H. R. (1980) *Biochemistry 19*, 5303–5309.

Hanson, S., McCartan, K., Sabina, R. L., Holmes, E. W., & Ullman, B. (1990) *J. Biol. Chem. 265*, 11474–11481.

Ikehara, M. (1973) *Chem. Pharm. Bull. (Tokyo) 21*, 444–445.

Jones, W., Kurz, L. C., & Wolfenden, R. (1989) *Biochemistry 28*, 1242–1247.

Kurz, L. C., Moix, L., Riley, M. C., & Frieden, C. (1992) *Biochemistry 31*, 39–48.
Long, R. A., Robins, R. K., & Townsend, L. B. (1967) *J. Org. Chem. 32*, 2751–2756.
Lowe, C. R. (1977) *Eur. J. Biochem. 73*, 265–274.
Lowenstein, J. M. (1972) *Physiol. Rev. 52*, 382–414.
Manfredi, J. P., & Holmes, E. W. (1984) *Arch. Biochem. Biophys. 233*, 515–529.
Martin, R. B. (1985) *Acc. Chem. Res. 18*, 32–38.
Merkler, D. J., & Schramm, V. L. (1987) *Anal. Biochem. 167*, 148–153.
Merkler, D. J., & Schramm, V. L. (1990) *J. Biol. Chem. 265*, 4420–4426.
Merkler, D. J., Wali, A. S., Taylor, J., & Schramm, V. L. (1989) *J. Biol. Chem. 264*, 21422–21430.
Merkler, D. J., Brenowitz, M., & Schramm, V. L. (1990) *Biochemistry 29*, 8358–8364.
Meyer, S. L., Kvalnes-Krick, K. L., & Schramm, V. L. (1989) *Biochemistry 28*, 8734–8743.
Morrison, J. F., & Uhr, M. L. (1966) *Biochim. Biophys. Acta 122*, 57–74.
Murakami, K. (1979) *J. Biochem. (Tokyo) 86*, 1331–1336.
Newby, A. C. (1984) *Trends Biochem. Sci. 9*, 42–44.
Nygaard, P. (1983) in *Metabolism of Nucleotides, Nucleosides, and Nucleobases in Microorganisms* (Munch-Petersen, A., Ed.) pp 54–64, Academic Press, New York.
Quinn, D. M., & Sutton, L. D. (1991) in *Enzyme Mechanism from Isotope Effects* (Cook, P. F., Ed.) pp 72–126, CRC Press, Boca Raton, FL.
Ronca, G., Bauer, C., & Rossi, C. A. (1967) *Eur. J. Biochem. 19*, 434–438.
Sabina, R. L., Fishbein, W. N., Pezeshkpour, G., Clarke, P. R. H., & Holmes, E. W. (1992) *Neurology 42*, 170–179.
Smolenski, R. T., Suitters, A., & Yacoub, M. H. (1992) *J. Mol. Cell. Cardiol. 24*, 91–96.
Streeter, D. G., Witkowski, J. T., Khare, G. P., Sidwell, R. W., Bauer, R. J., Robins, R. K., & Simon, L. N. (1973) *Proc. Natl. Acad. Sci. U.S.A. 70*, 1174–1178.
Szondy, Z., & Newsholme, E. A. (1989) *Biochem. J. 261*, 739–742.
Weiss, P. M., Cook, P. F., Hermes, J. D., & Cleland, W. W. (1987) *Biochemistry 26*, 7378–7384.
Wilson, D. K., Rudolph, F. B., & Quiocho, F. A. (1991) *Science 252*, 1278–1284.
Wolfenden, R., Kaufman, J., & Macon, J. B. (1969) *Biochemistry 8*, 2412–2415.
Yeung, C. Y., Ingolia, D. E., Roth, D. B., Shoemaker, C., Al-Ubaidi, M. R., Yen, J. Y., Ching, C., Bobonis, C., Kaufman, R. J., & Kellems, R. E. (1985) *J. Biol. Chem. 260*, 10299–10307.
Yoshino, M., & Murakami, K. (1980) *Biochim. Biophys. Acta 616*, 82–88.
Yoshino, M., & Murakami, K. (1981) *Biochim. Biophys. Acta 672*, 16–20.
Yoshino, M., & Murakami, K. (1985) *Biochem. Biophys. Res. Commun. 129*, 287–292.
Yoshino, M., & Murakami, K. (1986) *Int. J. Biochem. 18*, 235–239.
Yoshino, M., & Murakami, K. (1988) *Biochim. Biophys. Acta 954*, 271–276.
Yoshino, M., Murakami, K., & Tsushima, K. (1979) *Biochim. Biophys. Acta 570*, 157–166.
Yun, S.-L., & Suelter, C. H. (1978) *J. Biol. Chem. 253*, 404–408.
Zielke, C. L., & Suelter, C. H. (1971) *J. Biol. Chem. 246*, 1313–1317.
Zoref-Shani, E., Shainberg, A., & Sperling, O. (1983) *Biochem. Biophys. Res. Commun. 116*, 507–512.